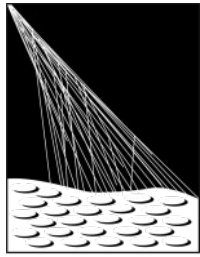


Anisotropies in the arrival directions of ultra-high-energy cosmic rays measured at the Pierre Auger Observatory

Teresa Bister
for the Pierre Auger Collaboration
RWTH Aachen University

New Frontiers in Physics
ICNFP 2020
08.07.2020



PIERRE
AUGER
OBSERVATORY



Ultra-high-energy Cosmic Rays

UHECRs:

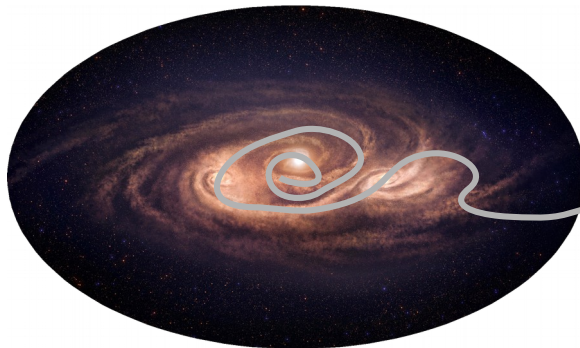
particles arriving at Earth
with energies 10^{18} eV to 10^{20} eV

open questions:

- *What are their sources?*
- *How are they accelerated?*
- *How do they propagate through the universe?*
- *What charges & masses do they have?*

current understanding:

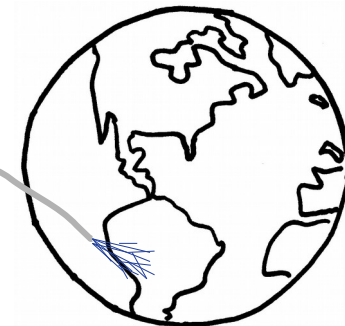
powerful extragalactic source
accelerates nuclei



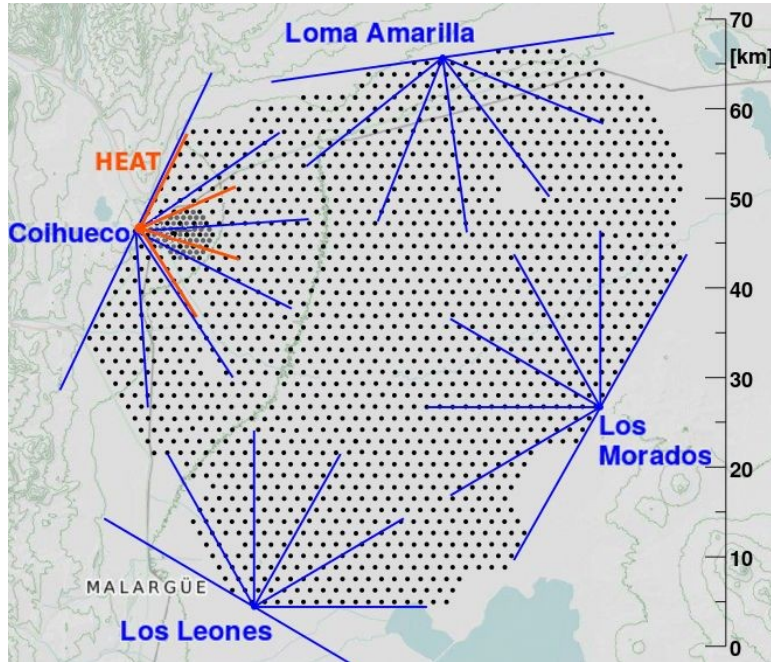
deflection
by cosmic magnetic fields



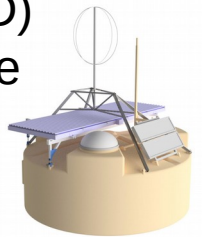
detection at Earth
by airshower



The Pierre Auger Observatory



- located near Malargüe, Argentina
- **largest UHECR detector world-wide:**
area of 3000 km²
- **hybrid detection:**
 - grid of 1600 + 60 water Cherenkov stations (SD)
→ 1500m / 750m grid, 100% duty cycle
 - 4 sites of fluorescence telescopes (FD)
→ 24 + 3 telescopes, ~15% duty cycle
- **update ongoing: AugerPrime**



Measurable quantities at Earth:

- shower depth → charge?
- energy of primary particle
- arrival direction

Cosmic ray composition: shower depth

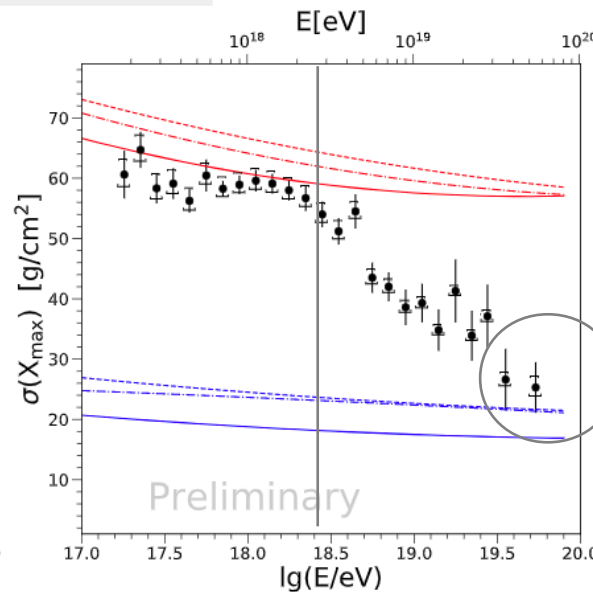
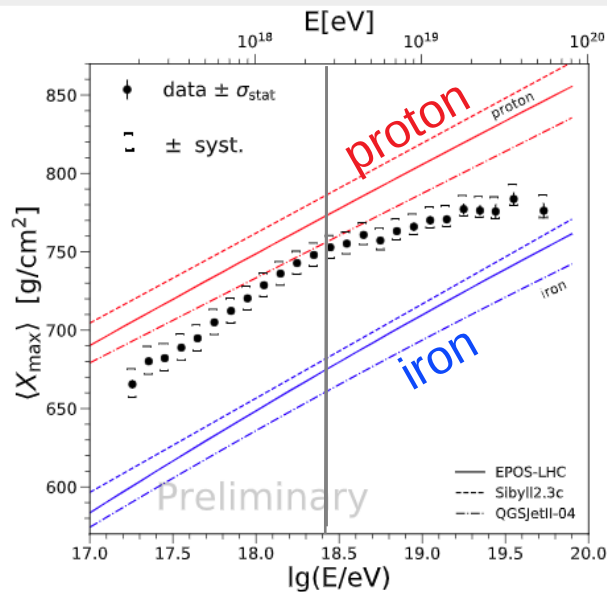
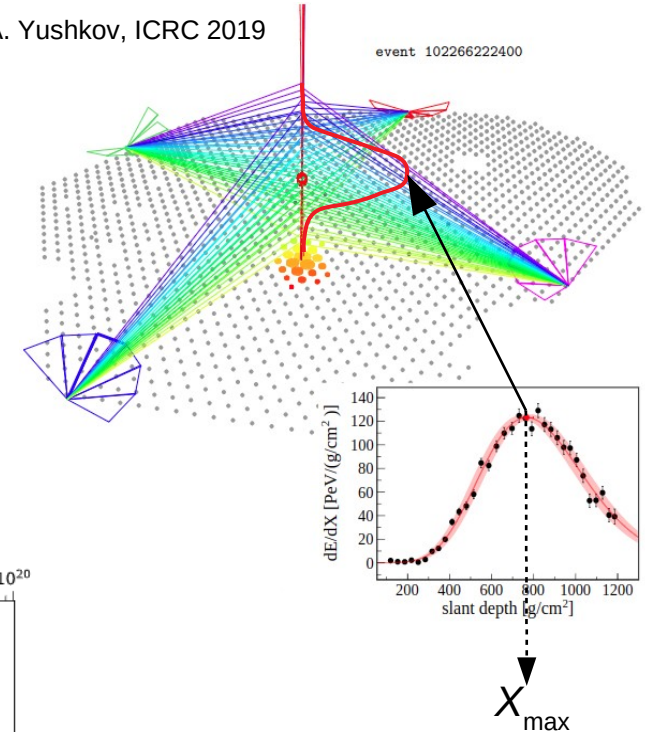
- shower depth X_{\max} : contains information about mass of primary particle
- reconstruction of longitudinal profile with the FD

below the ankle:
transition from light to heavy composition

above the ankle:
composition becomes heavier again

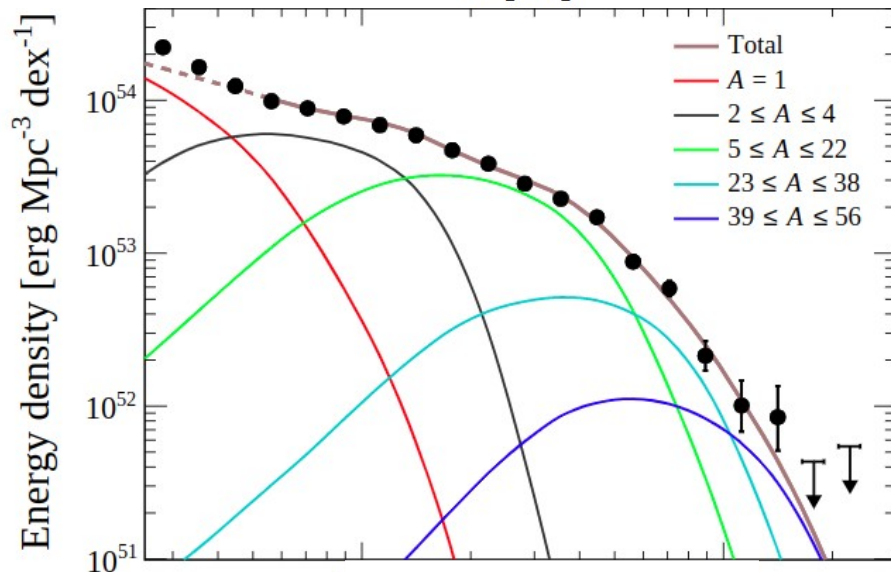
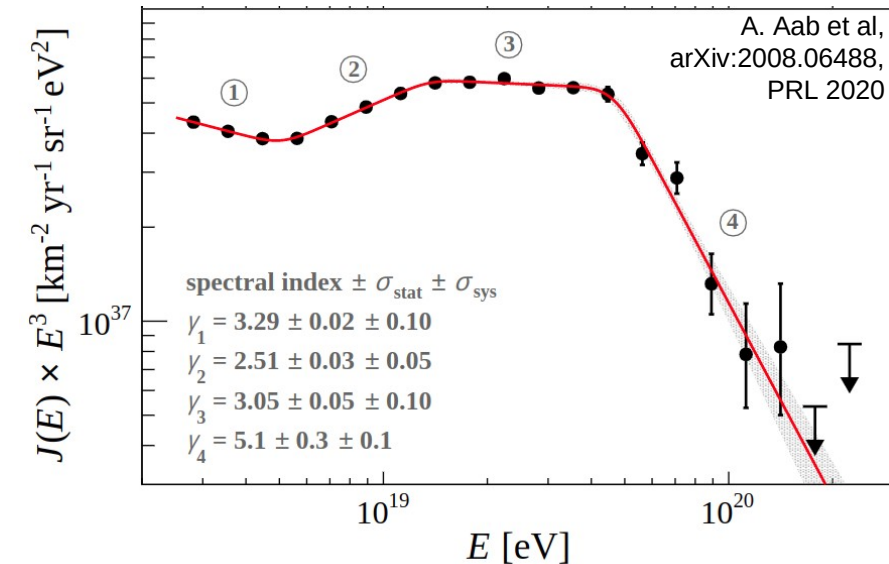


A. Yushkov, ICRC 2019



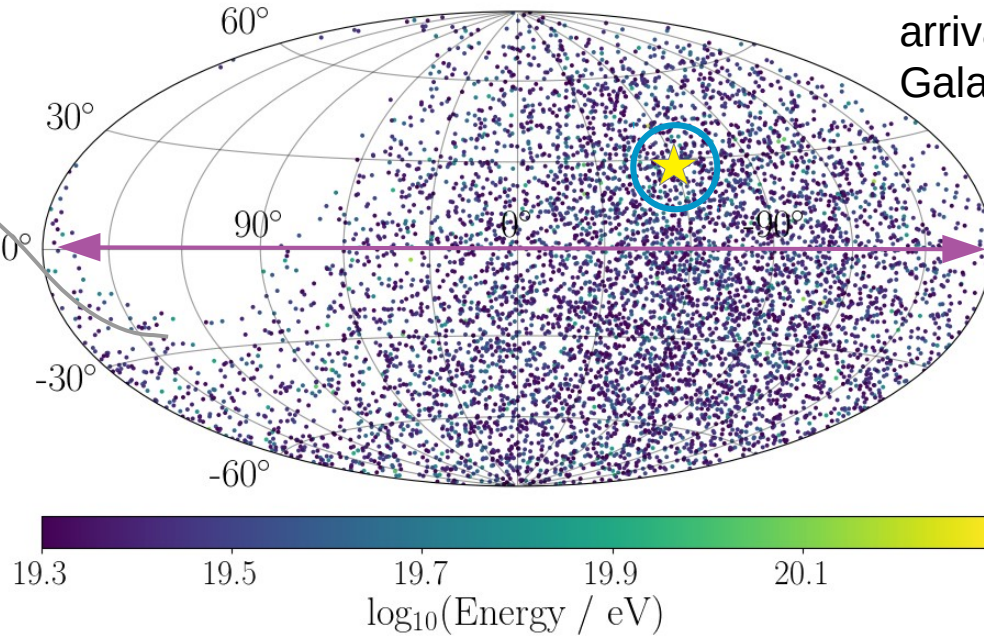
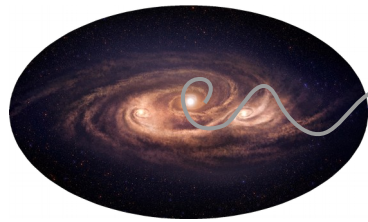
at the highest energies:
limited by 15% FD duty cycle

Cosmic ray energy spectrum



- **power law:** $J(E) \sim E^{-\gamma}$
 - fitted with 4 power laws, smooth transitions
- **features** at highest energies:
 - ankle ($5 \cdot 10^{18}$ eV) ① → ②
 - suppression at highest energies ② → ④
- **possible origin of suppression:**
 - maximum source energy?
 - propagation effect?
- **composition at highest energies?**

Cosmic ray arrival directions



deflection by magnetic fields

- magnetic field models inconsistent
- backtracking to source challenging task even with exact E & Z measurement

search for deviation from isotropy to investigate sources:

large scale anisotropies:

- *dipole* at energy > 8 EeV
- analysis method: Fourier analysis (harmonics in right ascension & azimuth)



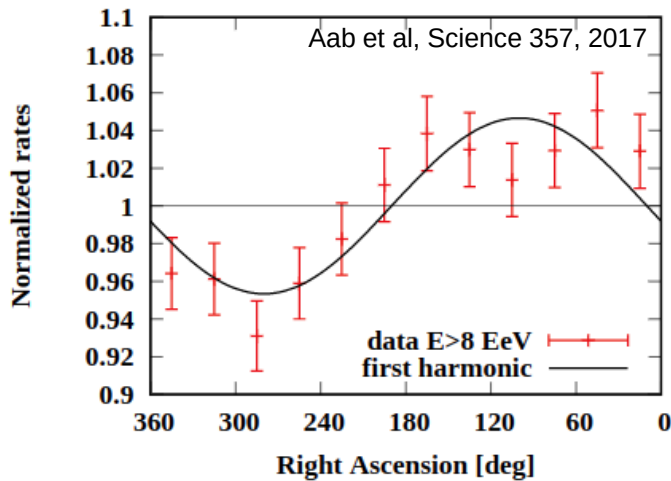
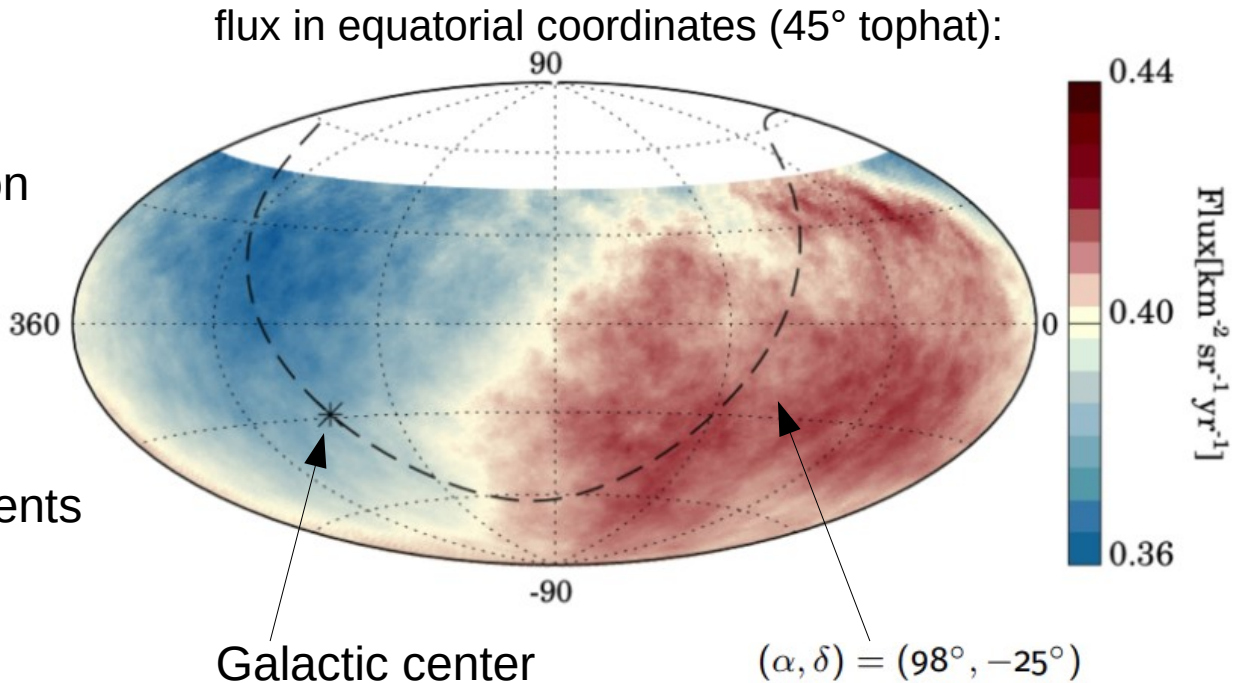
small & intermediate scale ($\lesssim 30^\circ$) anisotropies:

- at higher energies: less deflection expected
→ smaller angular scales
- methods: blind overdensity search, comparison to catalog sources...



Large scale anisotropy

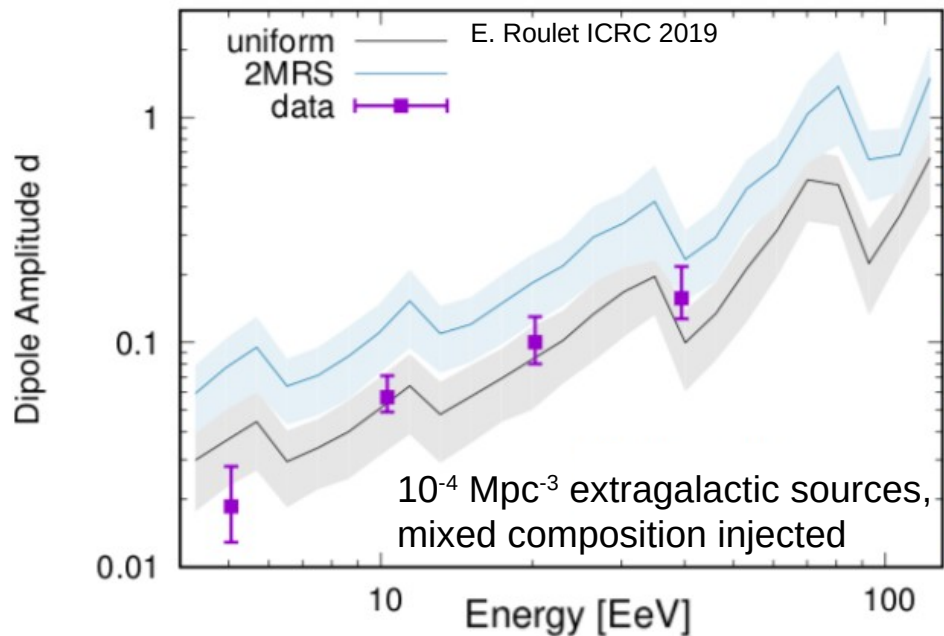
- first confirmed anisotropy in UHECR arrival directions
- harmonic analysis in right ascension → **dipolar modulation**
- **significance $> 5\sigma$**
- amplitude: $(6.6^{+1.2}_{-0.8})\%$
- no significant quadrupolar components



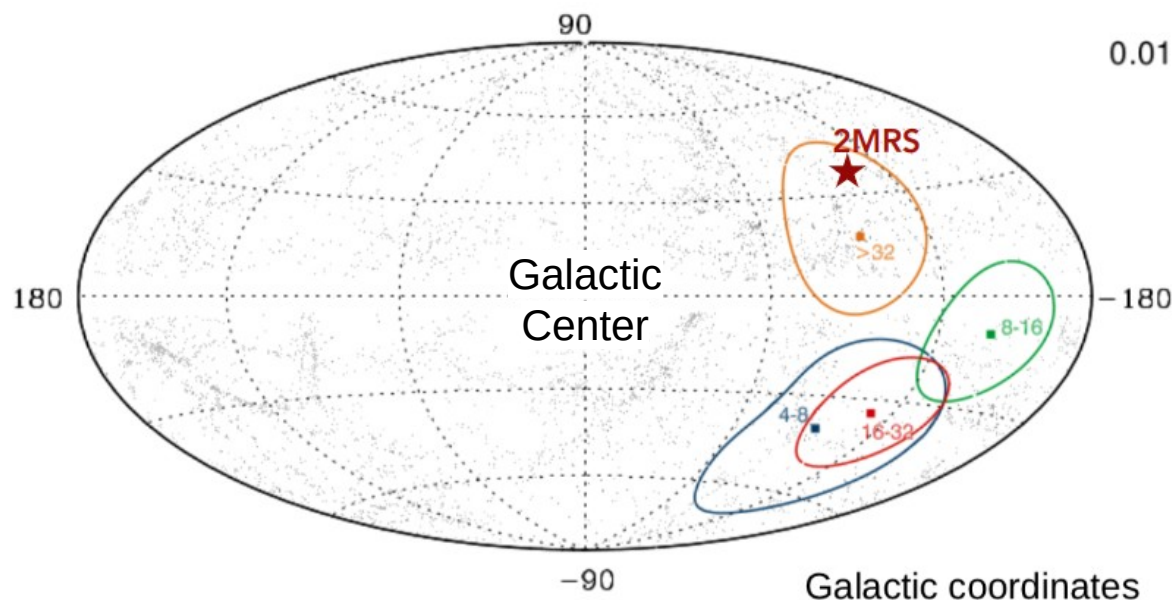
dipole points 125° away from Galactic center
→ indication for extragalactic origin of UHECRs

Energy dependency of the large scale anisotropy

- **dipole amplitude increases as function of energy:**
flat dependency excluded at 5.1σ
- energy dependence as expected



D. Harari et al., PRD92 (2015)

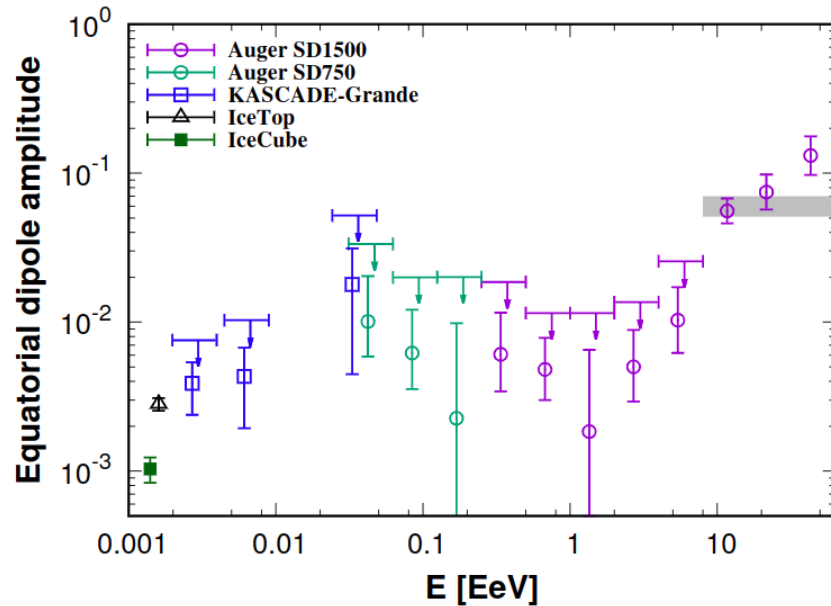


- dipole direction changes with energy
- close to mass center of 2MRS catalog & to outer spiral arm

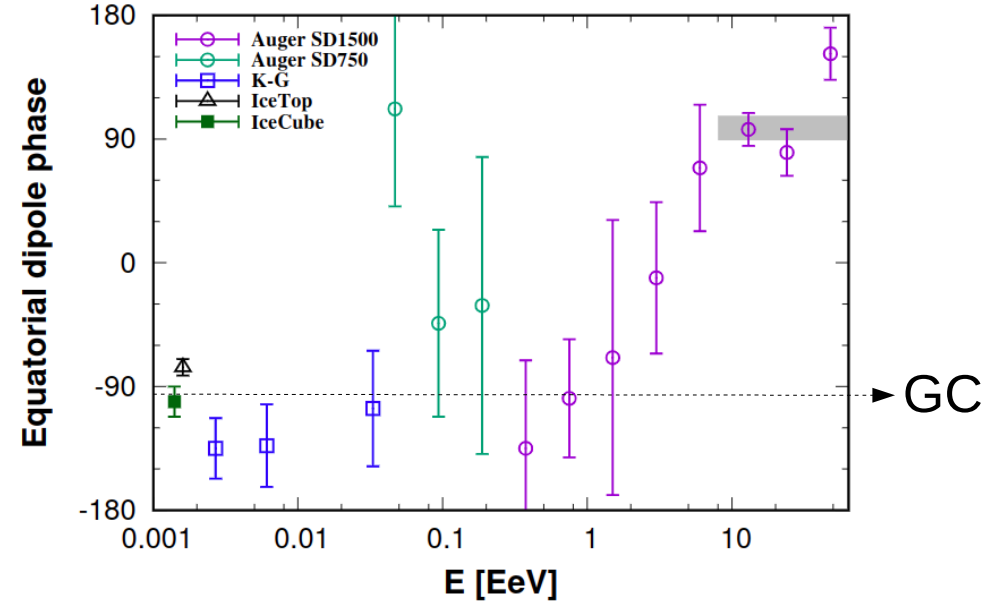
Extension to lower energies

extend dipole analysis to energies of 0.03 EeV

using SD 1500 & SD 750 & East-West method below 2 EeV



dipole amplitude increases with energy
from ~1% to ~6%
(lower amplitudes not significant)



phase changes from Galactic Center
at lower energies to opposite direction

→ **suggests transition from Galactic to extragalactic injection at few EeV**

Small & intermediate scale anisotropies

Analyses ICRC 2019: (Caccianiga ICRC 2019)

- model-independent **blind search** for overdensities
- overdensity search around **Centaurus A** region nearest radio-loud AGN, $d < 4$ Mpc
- **Likelihood test using 4 astrophysical catalogs:**
 - γ -emitting Active Galactic Nuclei (AGNs)
 - selection of starburst galaxies
 - Swift-BAT AGNs
 - 2MRS (traces local matter)

dataset:

- largest dataset so far:
01.01.2004 – 31.08.2018
- energies above 32 EeV
- total exposure 101,400 km² sr yr
- 2157 events from water Cherenkov array



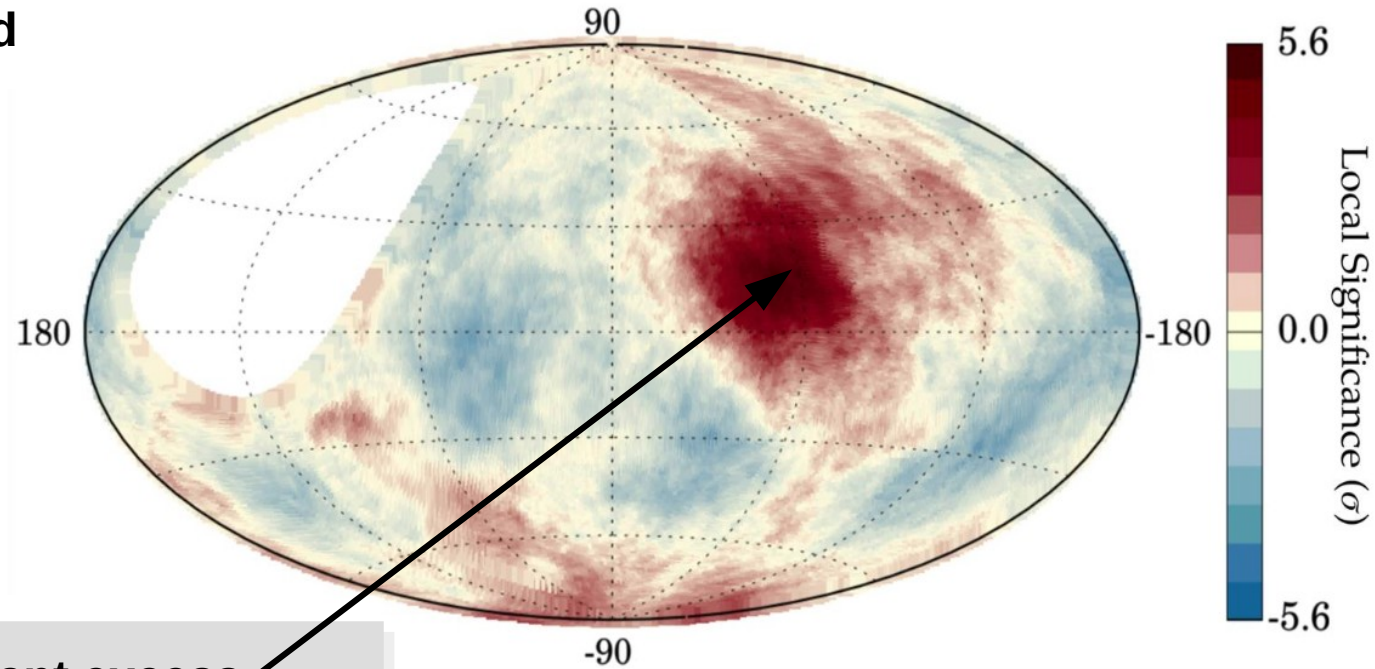
Centaurus A (AGN)



SBG

Blind search for overdensities

- **blind search on $1^\circ \times 1^\circ$ grid**
- 2 scan parameters:
 - energy threshold
 $32 \text{ EeV} \leq E_{\text{th}} \leq 80 \text{ EeV}$
 - circular window size
 $1^\circ \leq \psi \leq 30^\circ$



most significant excess:

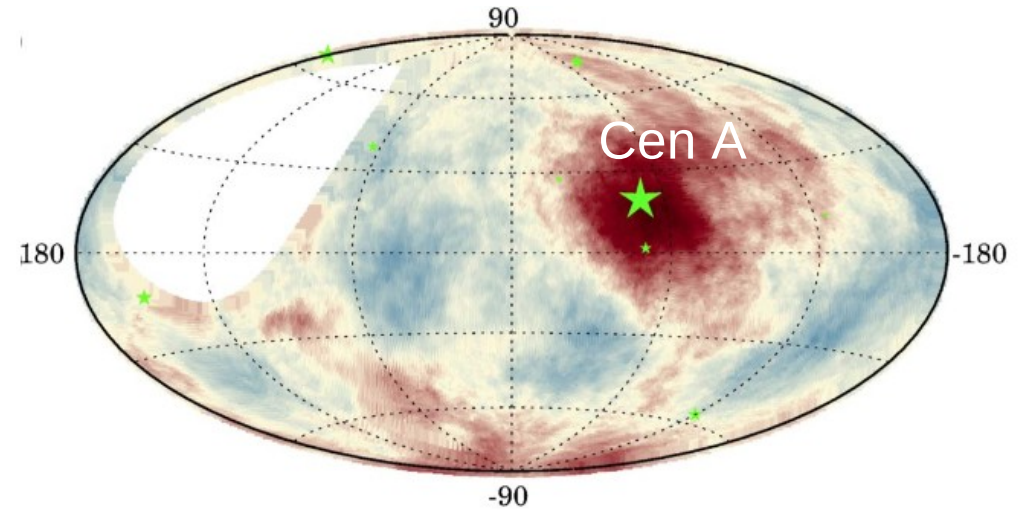
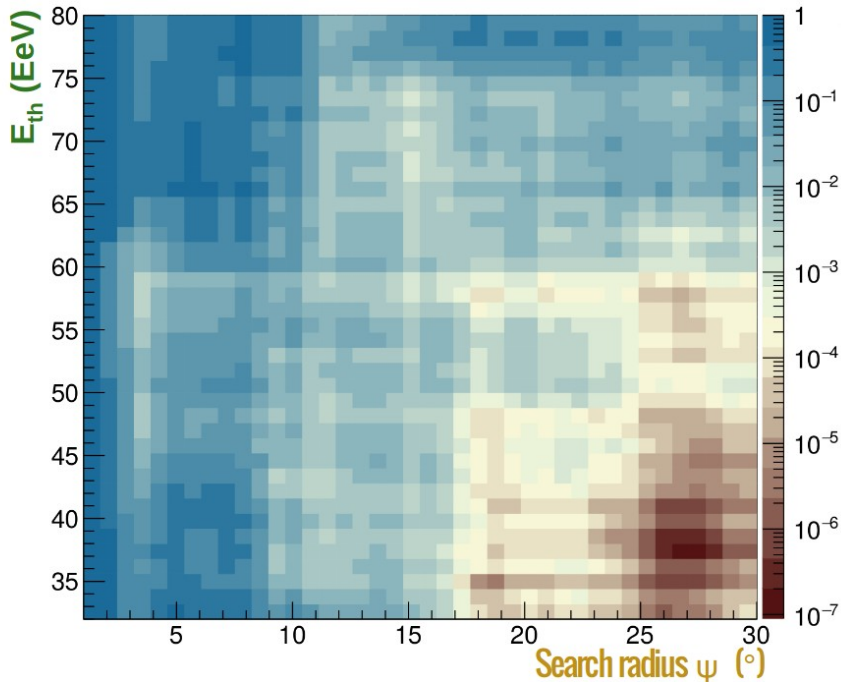
$E_{\text{th}} = 38 \text{ EeV}$, $\psi = 27^\circ$,

local Li-Ma significance 5.6σ ,

post-trial **p=2.5%**

Correlation with the direction of Centaurus A

- 2 scan parameters:
 - energy threshold
 $32 \text{ EeV} \leq E_{\text{th}} \leq 80 \text{ EeV}$
 - circular window size
 $1^\circ \leq \psi \leq 30^\circ$



significance:

$$E_{\text{th}} = 37 \text{ EeV}, \psi = 28^\circ,$$

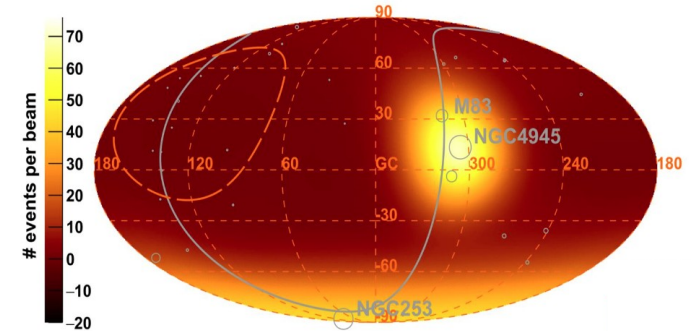
local significance 5.1σ ,

post-trial **3.9σ**

Likelihood comparison to astrophysical catalogs

- Compare data to probability maps via **Likelihood**
- **two free parameters:**
 - source fraction f_{aniso}
(fraction coming from catalog sources, rest isotropically distributed)
 - smearing angle θ (magnetic fields)
- scan of energy threshold
 $32 \text{ EeV} < E_{\text{th}} < 80 \text{ EeV}$ (1 EeV steps)
- weight catalog objects with relative flux in electromagnetic wavelengths
- **test statistic (likelihood ratio):**
$$\text{TS} = 2 \log [L(f_{\text{aniso}}, \theta) / L(f_{\text{aniso}}=0)]$$

probability map: starburst galaxies



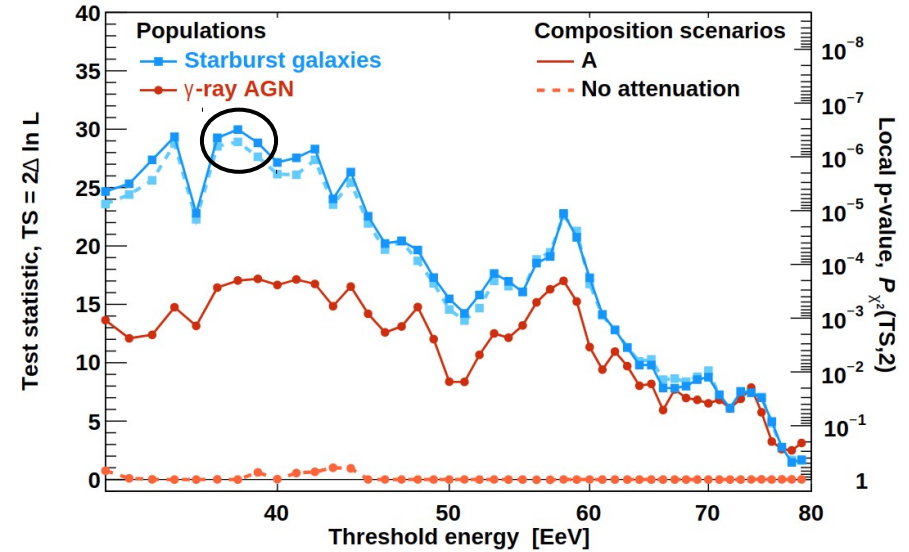
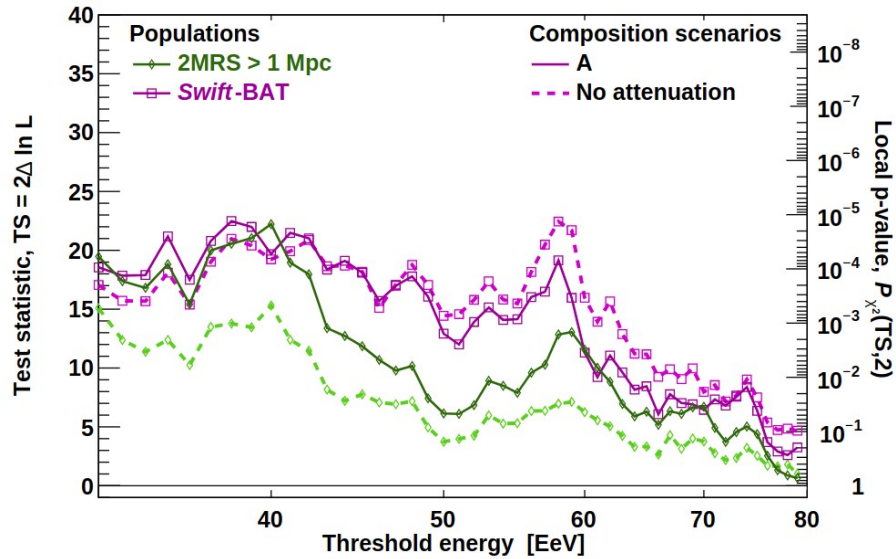
(Caccianiga ICRC 2019)

Catalog	E_{th}	θ	f_{aniso}	TS	Post-trial
Starburst	38 EeV	$15^{+5}_{-4}^\circ$	$11^{+5}_{-4}\%$	29.5	45σ ←
γ-AGNs	39 EeV	$14^{+6}_{-4}^\circ$	$6^{+4}_{-3}\%$	17.8	3.1σ
Swift-Bat	38 EeV	$15^{+6}_{-4}^\circ$	$8^{+4}_{-3}\%$	22.2	3.7σ
2MRS	40 EeV	$15^{+7}_{-4}^\circ$	$19^{+10}_{-7}\%$	22.0	3.7σ

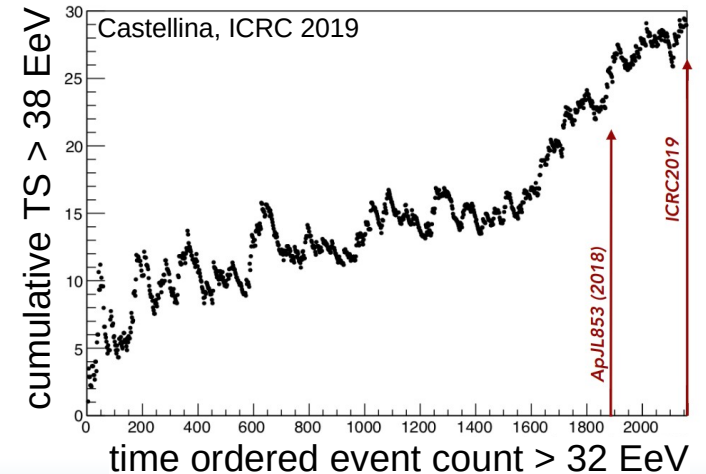
- all ~same angular scale & energy
- TS highest for starburst galaxies

Likelihood comparison to astrophysical catalogs

threshold energy scan:



- highest TS overall is 29.5 for starburst galaxies at energy threshold $E_{th} = 38$ EeV
- significance is increasing over time!



Summary

- **Pierre Auger Observatory:**

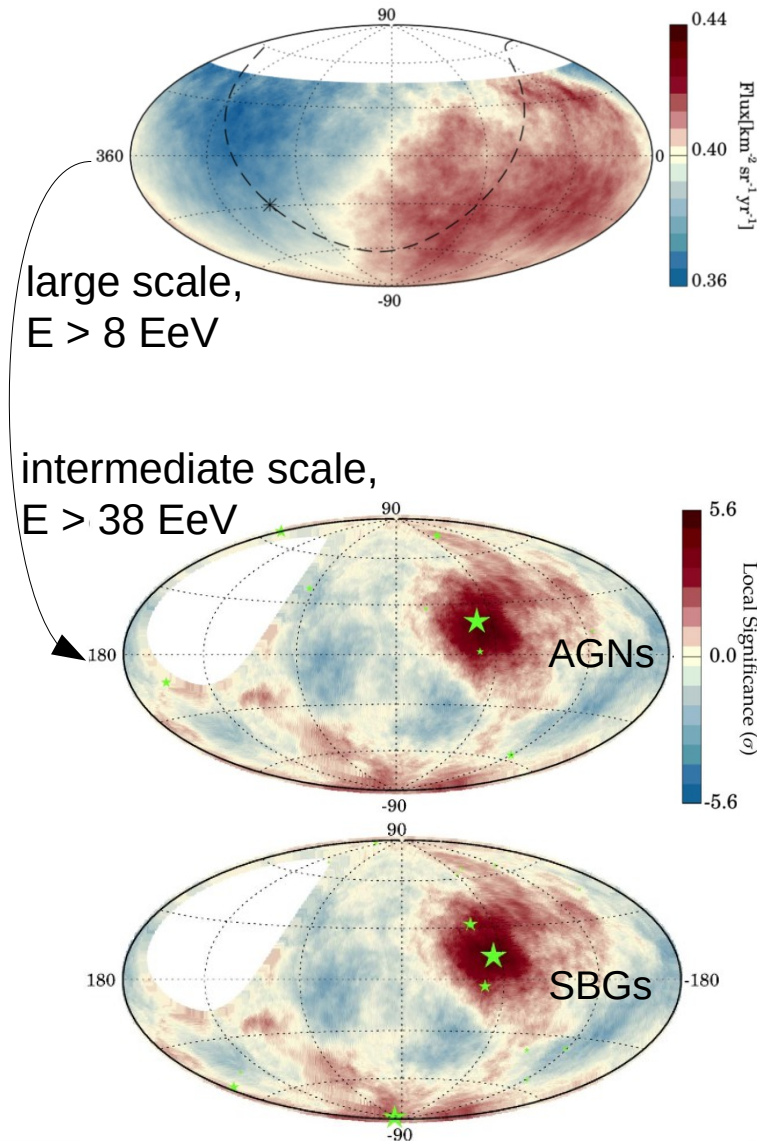
- largest detector to measure energy spectrum, composition & arrival directions of ultra-high-energy cosmic rays

- **large scale anisotropy:**

- **dipolar modulation** found with $> 5\sigma$ at $E > 8 \text{ EeV}$
- points 125° from Galactic center, amplitude increasing with energy

- **intermediate scale anisotropy:**

- all-sky blind search: no significant excess
- Centaurus A region: 3.9σ excess
- catalog comparisons:
 4.5σ correlation with starburst galaxies
with $E > 38 \text{ EeV}$, 15° angular scale



Future Perspectives

- confirm sources of ultra-high-energy cosmic rays
- study origin of flux suppression at highest energies
- select light particles for charged particle astronomy
- extend operations > 2025, upgrade to AugerPrime



backup

Likelihood test for anisotropy with astrophysical catalogs

γ -emitting AGNs

- Selected using Fermi 3FHL (was 2FHL)
- UHECR flux proxy: $\Phi(E > 10 \text{ GeV})$
- 33 sources (including Cen A, Fornax A, M87, Mkn421)
- Majority blazars of BL-Lac type and radio-galaxies of FR-I type

Swift-BAT

- UHECR flux proxy: $\Phi(14-195 \text{ keV})$
- Different AGN sample than previous one (both radio loud and quiet)
- >300 sources

Starburst Galaxies

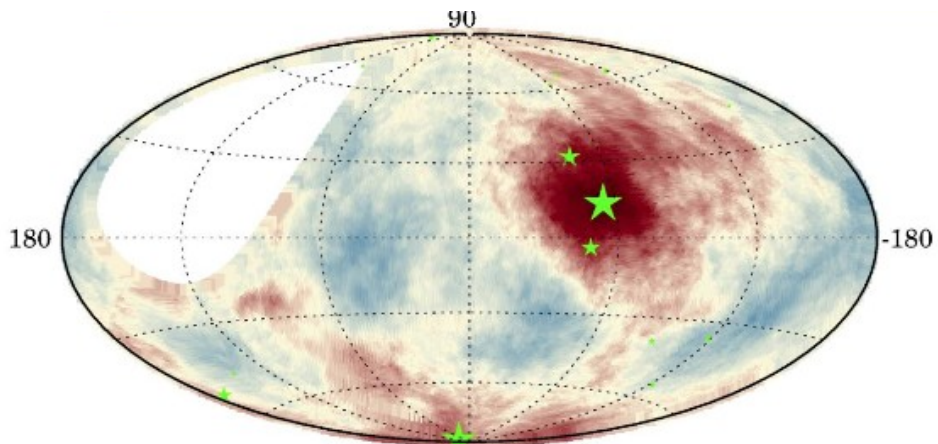
- UHECR flux proxy $\Phi(1.4 \text{ GHz})$
- Selection based on *Ackermann+ 12* and *Becker+ 09*, with the addition of data from HEASARC Radio Master Catalog
- 32 sources (including Circinus, M82, M83...)

2MRS

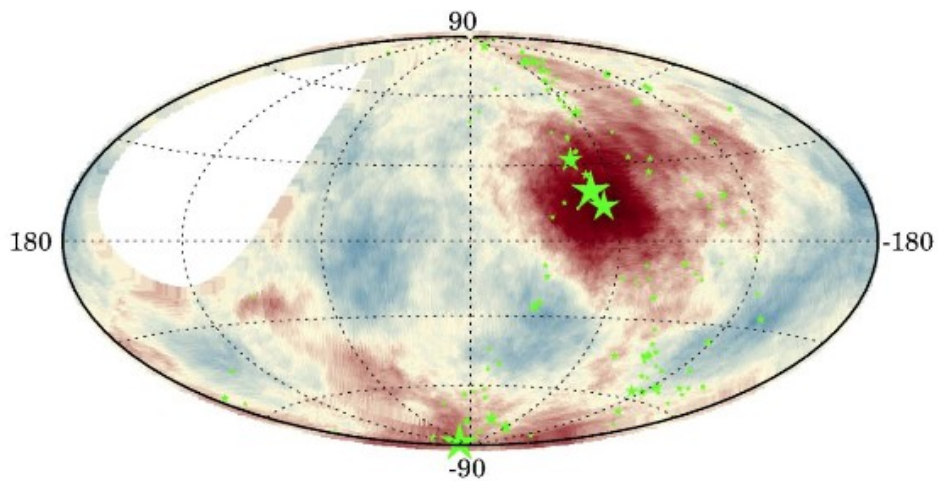
- UHECR flux proxy $\Phi(k\text{-band})$
- Traces local matter (some 10^4 sources)
- Local group taken away by selecting only events with $D > 1 \text{ Mpc}$

More details about catalog selection in ApJL, 853:L29 (2018)

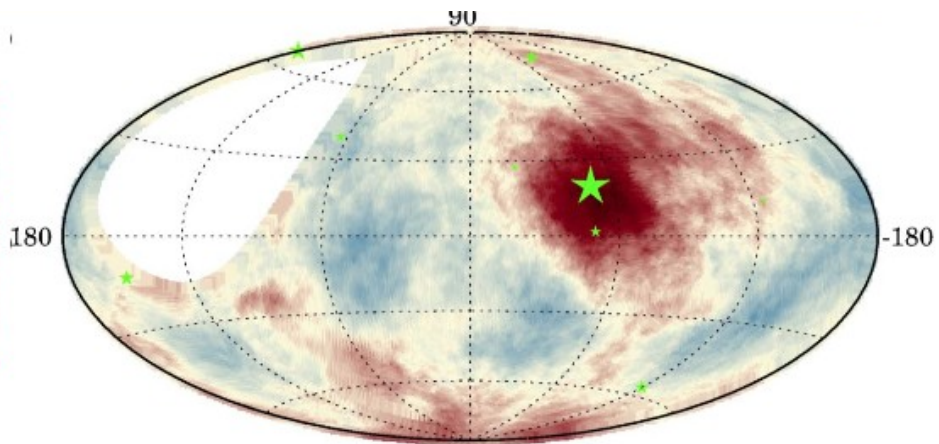
Starburst Galaxies



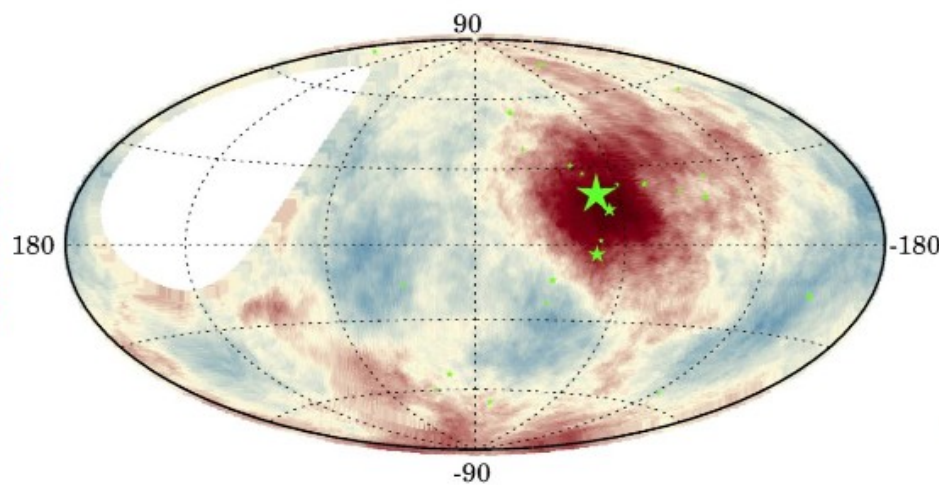
2MRS



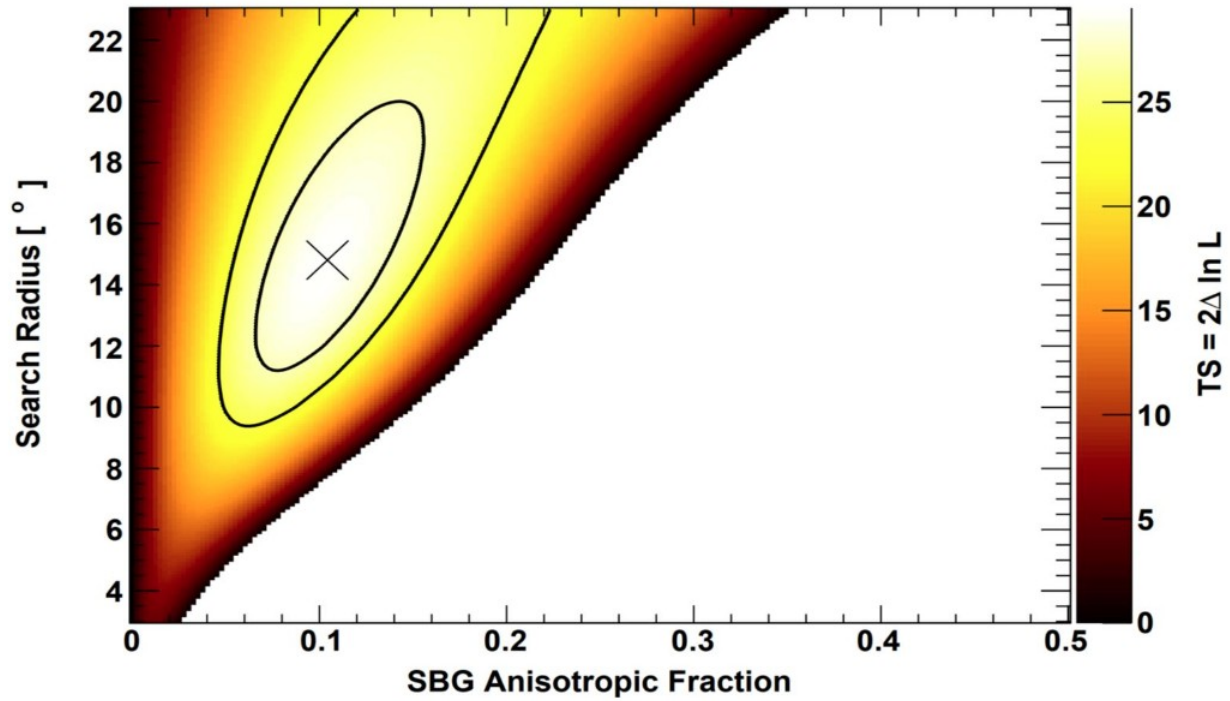
γ -emitting AGNs



Swift-BAT



Starburst galaxies - $E > 38 \text{ EeV}$



Sources most contributing to the likelihood analysis

Starburst Galaxies

Src	l	b	excess-weight
NGC4945	305.27	13.34	100.0%
NGC253	97.36	-87.97	77.7%
M83	314.58	31.97	27.7%
Circinus	311.33	-3.81	22.4%
NGC1068	172.10	-51.93	14.8%
NGC1808	241.21	-35.90	3.8%
NGC1672	268.78	-38.99	2.8%
NGC4631	142.81	84.22	2.2%
NGC1365	237.96	-54.60	2.1%
NGC4666	299.54	62.37	1.3%
M61	284.37	66.28	1.3%
NGC3627	241.96	64.42	1.3%
NGC2903	208.71	44.54	1.2%
M51	104.85	68.56	1.1%
NGC660	141.61	-47.35	1.1%
NGC3628	240.85	64.78	1.1%

γ -emitting AGNs

Src	l	b	excess-weight
CenA	309.52	19.42	100.0%
Mkn421	179.83	65.03	22.6%
NGC1275	150.58	-13.26	14.2%
FomaxA	240.16	-56.69	11.0%
M87	283.78	74.49	11.0%
CenB	309.72	1.73	7.3%
Mkn501	63.60	38.86	5.7%
APLibrae	340.68	27.58	2.3%
PMNJ0816-1311	234.80	12.12	1.6%

Swift-BAT

Src	l	b	excess-weight
CenA	309.52	19.42	100.0%
Circinus	311.33	-3.81	18.0%
NGC4945	305.27	13.34	12.9%
NGC2110	212.93	-16.55	3.8%
NGC6300	328.49	-14.05	3.3%
NGC5506	339.15	53.81	3.2%
MCG-05-23-016	262.74	17.23	3.0%
NGC7172	15.13	-53.07	2.5%
NGC3783	287.46	22.95	2.5%
NGC4507	299.64	22.86	2.1%
IC4329A	317.50	30.92	2.1%
NGC4388	279.12	74.34	2.1%
NGC7582	348.08	-65.70	1.9%
NGC4151	155.08	75.06	1.8%
ESO103-035	329.78	-23.18	1.4%
NGC1365	237.96	-54.60	1.4%
NGC6814	29.35	-16.01	1.3%
4U1344-60	309.77	1.51	1.3%
NGC3081	259.02	25.03	1.2%
NGC7314	27.14	-59.74	1.1%
NGC3227	216.99	55.45	1.1%
NGC3281	273.01	19.78	1.1%
NGC5728	337.32	38.10	1.1%
MCG-06-30-015	313.29	27.68	1.0%

Dipole amplitudes (ApJ 878, 2018)

Table 1: Dipole reconstruction for $E \geq 4$ EeV. Shown are the number of events in each bin N , the Equatorial amplitude d_{\perp} , the one along the rotation axis of the Earth d_z , and the total 3D amplitude d , as well as the dipole direction (α_d, δ_d) .

Energy [EeV]		N	d_{\perp}	d_z	d	α_d [°]	δ_d [°]
interval	median						
4 - 8	5.0	88,325	$0.010^{+0.007}_{-0.004}$	-0.016 ± 0.009	$0.019^{+0.009}_{-0.006}$	69 ± 46	-57^{+24}_{-20}
≥ 8	11.5	36,928	$0.060^{+0.010}_{-0.009}$	-0.028 ± 0.014	$0.066^{+0.012}_{-0.008}$	98 ± 9	-25 ± 11
8 - 16	10.3	27,271	$0.056^{+0.012}_{-0.010}$	-0.011 ± 0.016	$0.057^{+0.014}_{-0.008}$	97 ± 12	-11 ± 16
16 - 32	20.2	7,664	$0.075^{+0.023}_{-0.018}$	-0.07 ± 0.03	$0.10^{+0.03}_{-0.02}$	80 ± 17	-44 ± 14
≥ 32	39.5	1,993	$0.13^{+0.05}_{-0.03}$	-0.09 ± 0.06	$0.16^{+0.06}_{-0.03}$	152 ± 19	-34^{+19}_{-20}

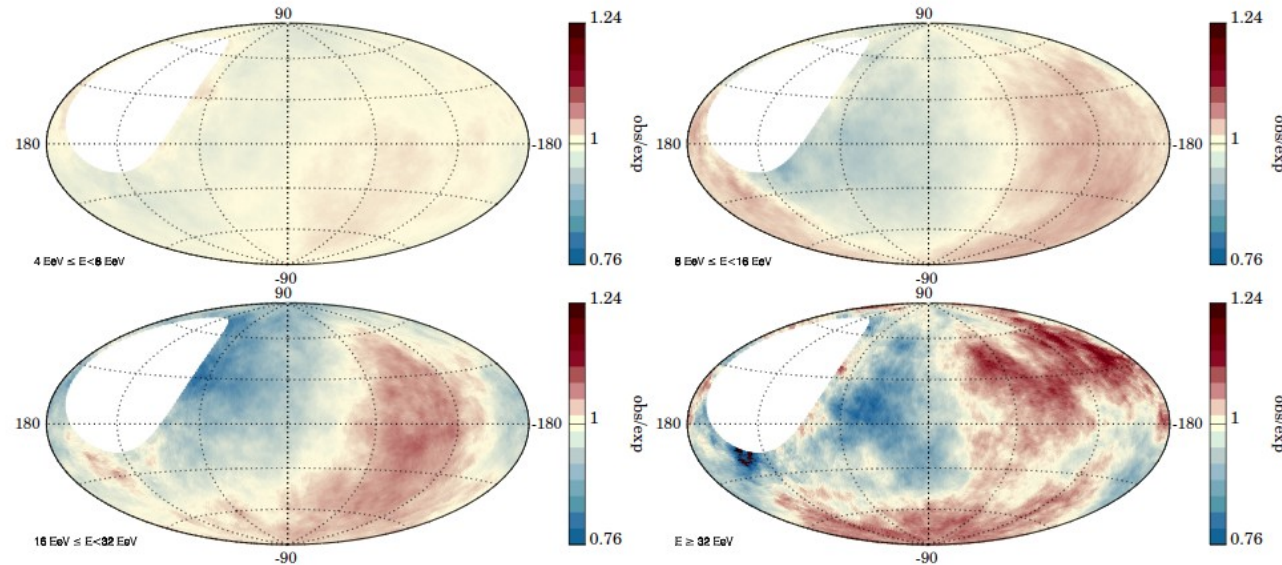


Figure 4. Maps in Galactic coordinates of the ratio between the number of observed events in windows of 45° over those expected for an isotropic distribution of arrival directions, for the four energy bins above 4 EeV.